Atmos. Chem. Phys. Discuss., 14, 26187–26230, 2014
www.atmos-chem-phys-discuss.net/14/26187/2014/
doi:10.5194/acpd-14-26187-2014

Atmospheric Chemistry and Physics Discussions

Primary marine aerosol emissions from the Mediterranean Sea during pre-bloom and oligotrophic conditions: correlations to seawater chlorophyll *a* from a mesocosm study

A. N. Schwier[1], C. Rose[1], E. Asmi[1,*], A. M. Ebling[2], W. M. Landing[2], S. Marro[3,4], M.-L. Pedrotti[3,4], A. Sallon[3,4], F. Iuculano[5], S. Agusti[5,6], A. Tsiola[7], P. Pitta[7], J. Louis[3,4], C. Guieu[3,4], F. Gazeau[3,4], and K. Sellegri[1]

[1]Laboratoire de Météorologie Physique CNRS UMR6016, Observatoire de Physique du Globe de Clermont-Ferrand, Université Blaise Pascal, 63171 Aubière, France
[2]Department of Earth, Ocean, and Atmospheric Science, Florida State University, Tallahassee FL 32306–4520, USA
[3]Laboratoire d'Océanographie de Villefranche (LOV), CNRS UMR7093, Observatoire océanologique, 06230 Villefranche-sur-mer, France
[4]Sorbonne Universités, UPMC Univ Paris 06, UMR7093, LOV, Observatoire océanologique, 06230 Villefranche-sur-mer, France

[5]Instituto Mediterráneo de Estudios Avanzados (IMEDEA CSIC-UIB), 07190 Esporles, Mallorca, Spain
[6]The UWA Oceans Institute and School of Plant Biology, University of Western Australia, 35 Stirling Highway, Crawley 6009, Australia
[7]Hellenic Centre for Marine Research (HCMR), P.O. Box 2214, 71003 Heraklion, Crete, Greece
*now at: Finnish Meteorological Institute, P.O. Box 503, 00101, Helsinki, Finland

Received: 24 July 2014 – Accepted: 26 September 2014 – Published: 20 October 2014

Correspondence to: A. N. Schwier (a.schwier@opgc.univ-bpclermont.fr) and K. Sellegri (k.sellegri@opgc.univ-bpclermont.fr)

Published by Copernicus Publications on behalf of the European Geosciences Union.

ACPD
14, 26187–26230, 2014

Abstract

The effect of ocean acidification and changing water conditions on primary marine aerosol emissions is not well understood on a regional or a global scale. To investigate this effect as well as the indirect effect on aerosol that changing biogeochemical parameters can have, ~52 m^3 pelagic mesocosms were deployed for several weeks in the Mediterranean Sea during both winter pre-bloom and summer oligotrophic conditions and were subjected to various levels of CO_2 to simulate the conditions foreseen in this region for the coming decades. After seawater sampling, primary bubble-bursting aerosol experiments were performed using a plunging water jet system to test both chemical and physical aerosol parameters. Comparing results obtained during pre-bloom and oligotrophic conditions, we find the same four log-normal modal diameters (18.5, 37.5, 91.5, 260 nm) describing the aerosol size distribution during both campaigns, yet pre-bloom conditions significantly increased the number fraction of the second (Aitken) mode, with an amplitude correlated to virus-like particles, heterotrophic prokaryotes, TEPs, chlorophyll *a* and other pigments. Organic fractions determined from κ closure calculations for $D_p \sim 50$ nm were much larger during the pre-bloom period (64 %) than during the oligotrophic period (38 %), and the organic fraction increased as the particle size decreased. Combining data from both campaigns together, strong positive correlations were found between the organic fraction of the aerosol and chlorophyll *a* concentrations, heterotrophic and autotrophic bacteria abundance, and dissolved organic carbon (DOC) concentrations. As a consequence of the changes in the organic fraction and the size distributions between pre-bloom and oligotrophic periods, we find that the ratio of cloud condensation nuclei (CCN) to condensation nuclei (CN) slightly decreased during the pre-bloom period. The enrichment of the seawater samples with microlayer samples did not have any effect on the size distribution, organic content or the CCN activity of the generated primary aerosol. pCO_2 perturbations had little effect on the physical or chemical parameters of the aerosol emissions, with

ACPD
14, 26187–26230, 2014

larger effects observed due to the differences between a pre-bloom and oligotrophic environment.

1 Introduction

With oceans covering 71 % of the Earth's surface, sea salt aerosol comprises a large portion of the natural aerosol emissions, with an estimated contribution between 2000 and 10 000 Tg yr^{-1} for sizes $D_p < 20$ µm (Gantt and Meskhidze, 2013). Marine aerosol can be produced from primary processes (e.g. sea salt aerosol from breaking waves) and secondary processes (i.e. formation via chemical processing). These aerosols can then have a large impact upon the Earth's radiative budget through both direct effects, such as light scattering, and indirect effects, by becoming cloud condensation nuclei (CCN) and affecting cloud formation. Due to the large flux of marine aerosol into the atmosphere, it is critical to better understand and determine the physical and chemical properties of marine aerosol as a function of changing marine environment water conditions.

At wind speeds greater than 4 m s^{-1}, marine aerosol is primarily formed via bubble bursting from breaking waves; three main types of drops, film, spume and jet drops, are produced depending on the mechanism (Lewis and Schwartz, 2004). Based on the size of aerosol formed, the chemical composition ranges from primarily inorganic sea salt particles to particles rich in organic material, yet different studies have shown differing compositions over the same size range. Typically, particles $D_p > 1$ µm have been found to be largely sea salt whereas smaller particles $D_p < 1$ µm contain increasing concentrations of organic with decreasing diameter (Ault et al., 2013; Facchini et al., 2008; Keene et al., 2007; O'Dowd et al., 2004; Prather et al., 2013). For particles in the size range relevant to cloud formation (50–150 nm), some have found an absence of hygroscopic salts in particles below 200 nm (Bigg and Leck, 2008), while other studies have shown the presence of sea salt and other inorganic elements (Ault et al., 2013; Clarke et al., 2006; Murphy et al., 1998; Quinn and Bates, 2011). Marine organic species

ACPD
14, 26187–26230, 2014

remain largely uncharacterized (Benner, 2002) and organic concentrations can vary drastically throughout the water column, both temporally and spatially (Russell et al., 2010). Primary emissions can gain organics either as bubbles traverse through the water column or at the ocean surface from the organic rich microlayer (Barger and Garrett, 1970; Bigg and Leck, 2008; Blanchard, 1964; Blanchard and Woodcock, 1957; Garrett, 1967; Lion and Leckie, 1981; Matrai et al., 2008). The sea surface microlayer has been shown to exhibit physical, chemical and biological differences from oceanic subsurface water (Cunliffe et al., 2013).

The marine aerosol emission flux is characterized by different source functions, the number of aerosols by particle size by area by time (Lewis and Schwartz, 2004). These source functions are dependent on a number of physical parameters, dominated by wind speed and sea surface temperature, but are also affected by the sea state (wave height, shape, etc.) and salinity (Grythe et al., 2014). Aerosol emissions are also dependent on the chemical composition of the seawater due to the presence of a rich and varied mixture of organic material. These organics can affect the waters' ability to form whitecaps (Callaghan et al., 2012) and change bubble lifetime (Garrett, 1967). Large-scale marine aerosol source functions used in models have started to include sea water composition (Langmann et al., 2008; Spracklen et al., 2008; Vignati et al., 2010) by focusing on parameterizations of the correlation between surface water chlorophyll *a* (chl *a*) concentrations and aerosol organic fractions (O'Dowd et al., 2008; Rinaldi et al., 2013).

Previous studies have indicated changing size distribution with increasing organic material (Fuentes et al., 2010b; King et al., 2012; Sellegri et al., 2006). Sellegri et al. (2006) saw a log-normal mode amplitude shift towards smaller diameters with the addition of sodium dodecyl sulfate (SDS) to artificial seawater; Fuentes et al. (2010b) observed similar behavior in tests with artificial sea water and biogenic exudates, while King et al. (2012) saw an additional lognormal mode at 200 nm with the addition of organic material to artificial seawater. Water temperature has also shown an effect on aerosol size distribution and number concentration, though different groups have seen

ACPD
14, 26187–26230, 2014

varying trends. Mårtensson et al. (2003) saw increasing number concentrations for particles > 350 nm and decreasing concentrations for particles < 70 nm with increasing water temperature in measurements of synthetic seawater. For all diameters in between, there was no clear trend. Sellegri et al. (2006) compared artificial seawater at 4 and 23 °C and found that the lognormal modal diameters all decreased with decreasing water temperature. Zábori et al. (2012b) measured the size distribution of NaCl and succinic acid/NaCl aerosol produced from an impinging water jet over a temperature range from 0–16 °C and found that the temperature did not influence the size distribution, yet it did influence the magnitude of aerosols produced (increasing temperatures led to decreased aerosol production). The dominance of small particles (dry diameter 10–250 nm) decreased with increasing water temperature over the range 0–10 °C. Above 10 °C, total number concentrations were stable regardless of the temperature. Similar results were found testing winter Arctic Ocean water (Zábori et al., 2012a) and Baltic seawater (Hultin et al., 2011), though for the Baltic seawater, the number concentration continued to drop until a water temperature of ∼ 14 °C.

Concentrations of marine organic aerosol seem to be highly dependent on the biological productivity at the ocean surface, following a seasonal bloom cycle. Studies performed at Mace Head in the North Atlantic Ocean and Amsterdam Island in the Southern Indian Ocean determined that the organic concentrations as well as the organic:sea salt ratio were highest in the spring/summer and the lowest in the winter (Sciare et al., 2000, 2009; Yoon et al., 2007). Phytoplankton blooms lead to increased levels of organic material (OM), both dissolved and particulate (Ducklow et al., 1995), with dissolved organic carbon (DOC) concentrations often greater than 80 µM under bloom conditions (Hansell et al., 2009). Different studies have linked the total submicron organic mass fraction of sea spray aerosol to chl *a* levels observed by satellite (Albert et al., 2012; O'Dowd et al., 2008; Rinaldi et al., 2013; Vignati et al., 2010); other studies have shown that the organic mass fraction was correlated with dimethylsulfide (DMS) (Bates et al., 2012) or heterotrophic bacteria abundance (Prather et al., 2013) instead. Hultin et al. (2010) measured sea water at depths of 2 m during an ocean

ACPD
14, 26187–26230, 2014

cruise west of Ireland and did not observe a correlation between chl *a* and sea spray production, instead finding a relationship with dissolved oxygen. Rinaldi et al. (2013) found that the correlation between chl *a* and OM at Mace Head was higher than the correlation of colored dissolved organic material or sea-water particulate organic carbon; however, the optimum correlation between chl *a* and OM was observed with an eight day time lag for chl *a*, indicating a complex, indirect relationship between biological processes and transferable organic matter. Various studies have shown linear correlations between chl *a* concentrations and organic fraction (O'Dowd et al., 2008; Rinaldi et al., 2013); others have observed exponential fitting correlation (Gantt et al., 2011), a power fit correlation (Fuentes et al., 2011), or a Langmuir functional relationship correlation (Long et al., 2011).

The CCN activity of marine aerosol has been tested in various laboratory experiments. Fuentes et al. (2010a) determined a plunging water jet system to be the bubble generation method most representative of ambient marine aerosol. In a separate study, Fuentes et al. (2010b) collected seawater samples from the West African coast for CCN measurements with phytoplankton exudates and saw a shift towards higher number concentrations and lower diameters in samples with high biological material. They found a variable relationship between chl *a* concentrations and OM production, stating that organic enrichment might also be dependent on specific conditions of algal blooms. The same dataset showed an increase in critical supersaturation of 5–24 % for the samples with high biological material compared to artificial seawater (Fuentes et al., 2011). Moore et al. (2011) performed laboratory experiments with NaCl or artificial seawater in combination with SDS, *Synechococcus, Ostreococcus* or oleic acid and found that 100× the normal organic concentration still did not affect the CCN activity or cloud formation properties. King et al. (2012) tested artificial seawater with different organics (palmitic acid, sodium laurate, fructose, mannose, SDS) and found that the number concentration decreased with the presence of stronger surfactants, most likely due to surface layer stabilization. The CCN activity was dependent on the contribution of the varying salts in the particle phase rather than the organics. In re-

ACPD
14, 26187–26230, 2014

cent wave channel experiments with natural seawater, Prather et al. (2013) saw the activation diameter augment from 63 to 118 nm after a five-fold increase in bacteria abundance; the size distributions remained essentially unchanged (as did phytoplankton, chl *a* and total organic carbon (TOC) abundances and concentrations), leading to the notion that a change in the sea salt chemical composition (the number fraction mode) must have affected the activation diameter. During the same campaign, Collins et al. (2013) observed the hygroscopicity parameter, κ, reduce by 86 ± 5 % over the same time period as the bacterial increase.

It is still unclear how changing biogeochemical water conditions will affect properties of marine aerosol. Ocean acidification may impact the chemical composition of seawater by affecting marine viruses (Danovaro et al., 2011), pelagic and heterotrophic organisms (Riebesell and Tortell, 2011; Weinbauer et al., 2011), and non-calcifying organisms (Doney et al., 2009). In the remote ocean, DMS was predicted by modeling studies to be one of the main precursors for CCN in the marine boundary layer, and studies have shown that regional DMS emission changes could affect CCN sensitivity (Cameron-Smith et al., 2011; Woodhouse et al., 2013). Archer et al. (2013) found that in acidification of Arctic seawater, average concentrations of DMS decreased by up to 60 % at the lowest pH; inversely, concentrations of DMSP, the precursor to DMS, increased by up to 50 %. In particular, the Mediterranean Sea is a rich and complex marine environment, generally classified as an oligotrophic basin (Bosc et al., 2004; Durrieu de Madron et al., 2011) with maximum open sea area chlorophyll concentrations of 2–3 mg m^{-3}, though high biological activity occurs annually in parts of the western Mediterranean, including coastal France in the late winter and early spring (D'Ortenzio and Ribera d'Alcalà, 2009; Siokou-Frangou et al., 2010). Mediterranean marine aerosol remains relatively uncharacterized, and it is important to quantify the regional effects of ocean acidification. In this work, we collected water from three mesocosms deployed in the Mediterranean Sea over two campaigns during different seasons as part of the MedSeA and ChArMEx projects to test the effects of ocean acidification and changes

ACPD
14, 26187–26230, 2014

in the biogeochemistry of the sea water on the physical and chemical properties of primary marine aerosol including size distributions and CCN activity.

2 Materials and methods

2.1 Measurement sites and campaigns

Mesocosm experiments were performed during two intensive campaigns: the first, during summer oligotrophic conditions (hereafter referred to as non-bloom conditions), occurred from 22 June to 10 July 2012 at the Station de Recherches Sous-marines et Océanographiques in the Bay of Calvi (BC), Corsica; the second, performed during winter pre-bloom conditions, took place from 21 February to 5 March 2013 in the Bay of Villefranche (BV), France. The presence of pre-bloom and non-bloom conditions was confirmed by the order-of-magnitude difference in the average sea water chl *a* concentrations (chl $a_{BC,avg} = 0.069 \pm 0.009\,mg\,m^{-3}$, chl $a_{BV,avg} = 1.005 \pm 0.125\,mg\,m^{-3}$). Detailed site and experimental information for both campaigns can be found in Gazeau et al. (2014).

Briefly, the mesocosms used in this study (volume of $\sim 52\,m^3$) were fully described in Guieu et al. (2014). The mesocosms consisted of large bags made of two 500 µm thick films of polyethylene mixed with vinyl acetate (EVA, 19 %) with nylon meshing in between to allow maximum resistance and light penetration (HAIKONENE KY, Finland). Natural seawater was filtered through a mesh grid to remove large debris when deploying the mesocosms. In order to avoid actual atmospheric deposition, the mesocosms were covered with UV-transparent ETFE roofs, except during periods of sampling. In this way, transfer of rainwater/deposition was prevented, while preserving the sunlight irradiance of the mesocosms. The covers were elevated to ~ 10 cm above the top of the mesocosms, allowing air to circulate to avoid a confinement effect in the trapped water. Among nine deployed mesocosms, three remained unmodified as controls and six were modified in terms of pCO_2. The pCO_2 levels used were slightly different be-

ACPD
14, 26187–26230, 2014

tween the two campaigns, as a consequence of different ambient pCO_2 levels (i.e. ~ 450 vs. 350 µatm at BC and BV, respectively). In the Bay of Calvi, the six targeted elevated pCO_2 levels were 550, 650, 750, 850, 1000 and 1250 µatm. In the Bay of Villefranche, the levels were 450, 550, 750, 850, 1000 and 1250 µatm. These elevated pCO_2 levels were reached by adding varying volumes of CO_2 saturated seawater to the mesocosms. At both sites, seawater was pumped from near the mesocosms and sieved onto a 5 mm mesh sieve in order to remove large organisms. Pure CO_2 was actively bubbled through the water for several minutes in order to achieve saturation; the water was then transferred to 25 L plastic containers for addition to the mesocosms. Depending on the targeted pCO_2 level, 50 L to more than 500 L were added. A diffusing system was used to ensure a perfect mixing of this CO_2 saturated seawater inside the mesocosms. In order to minimize the stress induced by the addition of large quantities of acidified water, the acidification of the mesocosms was performed over 4 days, and the experiments started when the targeted pCO_2 levels were reached.

For the experiments described here, every morning approximately 5 L of surface (~ 15 cm) water was pumped from each mesocosm using a PFA pump (St-Gobain Performance Plastics) activated by the pressurized air from a diving tank and connected to braided PVC tubing (Holzelock-Tricoflex, I.D. 9.5 mm). The water pump was flushed with seawater from the respective mesocosm prior to sampling. Samples were stored in large brown glass bottles outside (avoiding direct sunlight) until the experiments were performed that same day. During the BV campaign, the pump could not be used on 3 March 2013 due to unsafe sea conditions; water was instead manually sampled from the mesocosms with 2.5 L glass bottles while wearing long gloves. Additionally, due to dangerous wind and wave conditions, sampling was not performed on 5 March 2013 during the BV campaign. Instrumental failures occurred on 4 and 10 July 2012 at BC and on 28 February–1 March 2013 at BV.

The mesocosms were reached via ocean kayak or boat. For both campaigns, sampling operations were performed from a mobile plastic platform that was moved via a rope network. The water temperature variances between BC and BV are quite dras-

ACPD
14, 26187–26230, 2014

tic, given the time of year the experiments took place. From CTD measurements, at BC the water temperature measured nearest to the surface varied from 21.8–25.2 °C; at BV, the temperatures ranged from 13.0–13.6 °C.

For the experiments described here, we focused on three different mesocosms: control mesocosm C3, and acidified mesocosms P3 and P6. Mesocosm P6 was the most acidified of all mesocosms ($pCO_2 \sim 1250$ µatm), and P3 was acidified to an intermediate level ($pCO_2 \sim 750$ µatm). This allowed a range of acidification effects to be analyzed.

2.2 Experimental methods

Bubble-bursting experiments were performed using a square glass tank (20 l × 20 w × 25 h cm), filled with 3.6 L of seawater (water depth of 10 cm), sealed with a stainless steel lid and continuously flushed with particle-free air (11 LPM). The tank was constantly slightly over-pressured with particle-free air to ensure the absence of ambient room air. Aerosols were generated by splashing mesocosm seawater through plunging water jets, separated into 8 jets via a flow distributor. The mesocosm seawater was re-circulated using a peristaltic pump; to minimize an increasing temperature of the seawater caused by constant re-circulation, a stainless steel heat exchanger was used on the seawater exiting the pump. The temperature of the water was recorded with a temperature sensor at the beginning and end of each experiment (for the BV campaign). Since no measurements of the bubble size distribution could be performed in such a small device, all water flow characteristics were performed according to the Fuentes et al. (2010a) settings, to reproduce the same bubble size distribution. The water flowrate was set to 1.8 LPM, the height of the jets above the water surface was 9 cm and the penetration depth of the jets was ~ 7.5 cm. Particle-free air was blown over the seawater (using a j shaped tube ~ 1.5 cm above the water surface) to mimic the wind blowing effect on the bubble-bursting process. Some of the water samples were also enriched by the addition of an organic rich microlayer from the same mesocosms (average 100 mL, range 50–170 mL). The enriched mesocosm

ACPD
14, 26187–26230, 2014

samples were tested after the un-enriched sample to compare the effect of additional organic species.

Blank measurements were performed during the first ten minutes of each experiment by verifying the aerosol concentration was zero in the particle-free air flushed tank. Between each water sample testing, the aquarium and tubing were rinsed with ultrapure water (> 18 MΩ), and clean water was re-circulated throughout the experimental setup for 10–15 min. Experiments were performed on the mesocosm water in different orders each day to make sure there were no experimental biases.

The aerosol flow was passed through a diffusion drier and was sent through a neutralizer into a differential mobility particle sizer (DMPS) and miniature continuous-flow streamwise thermal-gradient CCN chamber (CCNc) (Roberts and Nenes, 2005) to determine particle CCN activation properties. The neutralizer used was a variable-amplitude corona discharge which charges particles to the equilibrium charge distribution (Stommel and Riebel, 2004, 2005). For the BC experiments, the neutralizer voltage was ∼ 2.8 kV and for BV, ∼ 2.0 kV.

For the CCNc-DMPS system, aerosol flow passed first through a TSI-type DMA (length 44 cm) selecting particle sizes ranging from 10–400 nm by stepping the voltage. Immediately after the DMA, the aerosol flow was split between the CCNc and a TSI CPC model 3010. The DMA sheath flow rate was 9 LPM and the sample flow rate was 1 LPM in BC; 7.5 LPM and 1.35 LPM was used in BV, respectively. For the BV campaign, the aerosol flow was split 1 LPM for the CPC and 0.35 LPM to the CCNc. In the CCNc, a total aerosol flow rate of 100sccm with a sheath-to-aerosol flow ratio of 5 was used. The CCNc operated at specific temperature gradient (dT) settings, testing two different supersaturations (SS). For the BC campaign, a temperature gradient of 6° (dT6) was used in the column and the top temperature of the column varied as the ambient temperature changed ($T_{top} - T_{amb} = 2\,^{\circ}C$); in BV, d$T$6 and a temperature gradient of 3° (dT3) were tested and the top temperature of the column was always set at 30 °C. The data is plotted as activated fraction vs. particle diameter and fit with a sigmoid curve, from which we obtain the activation diameter at each dT (see Asmi et al., 2012

ACPD
14, 26187–26230, 2014

for more details). The CCNc system was calibrated with atomized $(NH_4)_2SO_4$ and NaCl solutions at the beginning, end and throughout each campaign. The activation diameter of the calibration was then used to calculate the corresponding supersaturation; this supersaturation was then used for all mesocosm experiments. The activation diameters and corresponding supersaturations for each dT are shown in Table 1.

2.3 Seawater parameters

Every day at 08:30 LT, depth-integrated sampling (0 to 10 m) was performed in each mesocosm using 5 L Hydro-Bios integrated water samplers. Samples for pigment analyses were filtered (2 L) onto GF/F. Filters were directly frozen with liquid nitrogen and stored at −80 °C. Measurements were performed on an HPLC from filters extracted in 100 % methanol, disrupted by sonication and clarified by filtration (GF/F Whatman). Samples for microbial diversity (2 mL) were fixed with 0.5 % final concentration glutaraldehyde, frozen in liquid nitrogen, and then transferred to a −80 °C freezer. Virus-like particles, heterotrophic and autotrophic prokaryotes abundances were measured with the use of Flow Cytometry (Beckton Dickinson FACS Calibur model). Total organic carbon (TOC) was measured instead of dissolved organic carbon (DOC) in order to avoid contamination during filtration. Due to the low concentration of particulate organic carbon in both sites (typically less than 10 % of TOC), it is referred to hereafter as DOC. DOC concentrations were determined on 20 mL samples by high temperature oxidation with a Shimadzu 5000 A TOC Analyzer. Transparent exopolymeric particles (TEPs) concentrations were measured spectrophotometrically according to a dye-binding assay (Engel, 2009). Samples (250 mL) were filtered onto 0.4 mm polycarbonate filters under low vacuum (< 100 mm Hg), stained with 1 mL of Alcian blue solution (0.02 g Alcian blue in 100 mL of acetic acid solution of pH 2.5) and rinsed with 1 mL of distillate water. Filters were then soaked for 3 h in 6 mL of 80 % sulfuric acid (H_2SO_4) to dissolve the dye, and the absorbance of the solution was measured at 787 nm, using acidic polysaccharide xanthan gum as a standard.

ACPD
14, 26187–26230, 2014

3 Results and discussion

In studying the effects of ocean acidification, it was necessary to observe whether changes with biogeochemical processes affected primary marine aerosol emissions and chemical and physical aerosol properties. For many of the parameters studied (e.g. chl *a* concentrations, total prokaryotic cells and virus-like particles abundances), there were no strong discernible differences between the control, C3, or the acidified mesocosms, P3 and P6, along the course of the experiments; however, there were often large differences between the two campaigns due to the pre-bloom and non-bloom conditions. In the following sections, we will relate trends observed with different biogeochemical parameters to those observed in the primary marine aerosol.

3.1 Aerosol size distributions and number concentration

The marine aerosol size distributions remained stable throughout the course of each campaign. Four lognormal modes were fit to the average size distributions of each campaign, with results summarized in Fig. 1 and Table 2. In order to investigate the size of the aerosol independently of the concentration, the size distributions were normalized using the total aerosol number concentration. The four lognormal modal diameters determined (~ 18.5, 37.5, 91.5, 260 nm) were present in both BC and BV. The lognormal mode fitting was also used to determine the particle number fraction at each lognormal modal diameter. Looking at the number fractions on a daily temporal scale for SS = 0.39 %, the lognormal mode number fractions remained relatively constant throughout both campaigns, though differences were noted between the campaigns (Fig. 2, Table 2). Throughout the campaign in BC, the fractions of Modes 1–3 were approximately equal in magnitude (~ 0.295), whereas in BV, the magnitude of the Mode 2 (the Aitken mode) fraction relative to the other modes was dominant (0.482). These same trends were observed for SS = 0.08 % and all the enriched mesocosm samples (Figs. 3–4). The increase in the Mode 2 particle fraction could be due to the presence of increased organic material, and thus increased number of organic particles,

ACPD
14, 26187–26230, 2014

at the smaller lognormal modal diameters. When augmenting the bacterial abundance in seawater, Collins et al. (2013) observed an increased particle fraction of the smallest lognormal mode diameter with no change to the shape or magnitude of the size distribution; this was attributed to the replacement of internally mixed salt/organic particle types by insoluble organic type particles. Previous studies have also indicated changing size distributions or mode number fractions with increasing organic material (Fuentes et al., 2010b; Sellegri et al., 2006).

Many other studies have found different lognormal mode distributions of both artificial and natural seawater samples, though many have similar modal sizes. Fuentes et al. (2010a) observed 4 modes (modal sizes 14, 48, 124, 334 nm) generated from plunging-water jet experiments with artificial seawater. Mode 4 was believed to be linked to splashing water from the jet mechanism. In a separate study (Fuentes et al., 2010b), 4 modes represented both artificial and natural seawater (modal sizes 15, 45, 125, 340 nm) well. Similar to our findings, increasing organic content was found to increase the number fraction of Mode 2 while decreasing the relative fractions of the other modes. In similar experiments with Baltic seawater collected between May and September, Hultin et al. (2011) observed either two lognormal modes (site: Askö, 86, 180 nm) or three lognormal modes (site: Garpen, 93, 193, 577 nm). Sellegri et al. (2006) tested synthetic sea salt with a weir and observed 3 lognormal modes (4 °C: 30, 85, 200 nm; 23 °C: 45, 110, 300 nm). After adding SDS, they noticed an increase in the fraction of particles at the smallest lognormal diameter. In synthetic seawater experiments with sintered glass filters, Mårtensson et al. (2003) observed one submicron lognormal mode (100 nm); Tyree et al. (2007) observed a lognormal mode at the same diameter using artificial and natural seawater with pore diffusers. The Mårtensson et al. (2003) and Tyree et al. (2007) studies using sintered glass filters or pore diffusers report relatively different size distributions compared to those obtained by plunging jet experiments, likely due to the bubble formation processes. Collins et al. (2013) observed three lognormal modes in seawater wave channel ex-

ACPD
14, 26187–26230, 2014

periments (∼ 90, 220, 1000 nm), with changing number fractions as described in the above paragraph.

Temperature has also been shown to affect size distributions and aerosol number concentrations (Hultin et al., 2011; Mårtensson et al., 2003; Zábori et al., 2012a). The initial and final water temperatures were measured over the course of an experiment (∼ 1 h, BV only); the water was found to increase by $4.6 \pm 1.2\,^{\circ}\mathrm{C\,h^{-1}}$ on average due to the constant water recirculation through the peristaltic pump and an insufficient heat exchange system (encompassing all experiments, water temperatures ranged from ∼ 11.7–26.8 °C from the initial to final measurement). This increase is 2–5× times higher than the 1–2 °C h^{-1} temperature increase measured by Zábori et al. (2012a). We observed that the increase in the water temperature only affected the magnitude of the size distribution, not the shape. However, there was no discernible clear correlation between the number concentration and average water temperature, in contrast to previous studies (Fig. 5). For any given experiment, the size distribution magnitude and the observed total number concentration increased, decreased or remained constant over the course of the BV campaign, indicating that the temperature effects could have been obscured by the natural variance of the plunging jet bubbling technique. Acidification had no effect on the aerosol size distribution or number concentration, as no clear differences were found between mesocosms C3, P3, and P6 within a given field campaign.

3.2 Activation diameter

By testing two temperature gradients, it is possible to look at the hygroscopic properties of different size particles based on the different supersaturations at which they are activated. The activation diameter time series measured at SS = 0.39 % (d*T*6) is shown in Fig. 6. In BC, there is little variation temporally between the control and acidified mesocosms tested ($D_{p,50,\mathrm{avg}} = 46.47 \pm 0.88$ nm), indicating that acidification does not have a large direct effect on CCN activity. Additionally, the enriched samples showed similar behavior to the non-enriched waters, indicating that the addition of the organic-

ACPD
14, 26187–26230, 2014

rich microlayer had little effect on the water uptake for the aerosols. For the experiments incorporating the enriched microlayer, the entire organic-rich volume was added a few minutes before starting the water jet system, rather than being continuously introduced to the tank throughout the entire experiment. This could have led to microlayer depletion over the course of an experiment, explaining why no visible difference was seen between the enriched and un-enriched samples. However, no clear difference was seen between the first (when the microlayer was present) and subsequent size distributions during a given microlayer enriched experiment. In past experiments, the addition of organics to bubbling experiments have shown changes in the size distribution (Sellegri et al., 2006), particle number concentration (Fuentes et al., 2010b; King et al., 2012; Tyree et al., 2007), and CCN activity (Collins et al., 2013; Fuentes et al., 2011). Other experiments have shown no visible changes (Moore et al., 2011) from the addition of organics, similar to the experiments performed in this study. In some studies, the concentrations and/or nature of some of the organic surfactants were unrealistic (King et al., 2012; Moore et al., 2011; Sellegri et al., 2006). At BV, there was much greater variability in the activation diameter for SS = 0.39 % over the course of the experiments ($D_{p,50,avg}$ = 59.48 ± 1.1 nm, Fig. 6), while at SS = 0.08 % the activation diameters were more stable ($D_{p,50,avg}$ = 141.91 ± 10.8 nm, Fig. 7). Activation diameters larger than the corresponding salt standards (here, shown as NaCl), indicating higher organic presence, are observed more at BV than BC for SS = 0.39 % due to the organic pre-bloom conditions, whereas the non-bloom water conditions were very stable at BC. For SS = 0.08 %, the activation diameters are very similar to the NaCl standard, which signifies a lower organic fraction for larger particles. Activation diameters for individual mesocosms in both campaigns are shown in Table 3.

There is an anti-correlation of the activation diameter at SS = 0.39 % with the ambient average air temperature in BV (Fig. 6), though no correlation exists with SS = 0.08 % (Fig. 7), or in BC (Fig. 6). However, more daily temperature variance was observed in BV than BC, based on the time of year of the campaigns. This anti-correlation could indicate an additional temperature impact on the emission of small particles (~ 50 nm)

ACPD
14, 26187–26230, 2014

and their chemical composition, though this effect is unclear and undocumented in the literature.

We investigated if the observed differences in the activation diameters from BC and BV could be linked to the different operating techniques used for the campaigns. As indicated previously, T_{top} in BC was variable, changing as the ambient temperature changed. As the ambient temperature changed throughout the day, the temperature in the column would also change, leading to possible temperature instabilities throughout the course of an experiment. On the contrary, in BV, T_{top} was fixed at 30 °C, a temperature higher than the daily temperature variability. In this way, temperature fluctuations in the column were avoided. However, in observing the measured temperatures throughout the column for both campaigns and all the experiments, the temperatures of the column remained quite stable for both methods of operation, so we believe that these effects are very minor. Additionally, it has been shown that organics can volatilize in the CCN column due to the temperature gradient (Asa-Awuku et al., 2009), biasing observed CCN activity. It is possible that this occurred for both campaigns based on the relatively high measured operating temperatures observed in the column; if organic material was volatilized, the activation diameters would increase from those shown here.

3.3 Kappa and organic fraction

The hygroscopicity of the aerosol was determined using kappa-Köhler theory (Petters and Kreidenweis, 2007) following Asmi et al. (2012). Using the activation diameter and numerical iteration, the kappa value was determined when the maximum of the saturation curve was equal to the supersaturation in the CCNc, following,

$$S(D_p) = \frac{D_p^3 - D_{p,50}^3}{D_p^3 - D_{p,50}^3(1-\kappa)} \exp\left(\frac{4\sigma_w M_w}{RT\rho_w D_p}\right) \quad (1)$$

ACPD
14, 26187–26230, 2014

where S is the supersaturation, D_p is the diameter of the droplet, $D_{p,50}$ is the dry diameter, R is the gas constant, T is temperature, and σ_w, M_w, and ρ_w are the surface tension, molecular weight and density of water, respectively. Lower kappa values correspond to more hydrophobic, or organic-like, particles. In BC, the average mesocosm kappa value at SS = 0.39 % was $\kappa_{avg,BC} = 0.95 \pm 0.17$, falling in the suggested range of the kappa average of marine aerosol, $\kappa_{marine} = 0.72 \pm 0.24$ (Pringle et al., 2010). In BV, the average mesocosm kappa values for SS = 0.39 % and 0.08 % are $\kappa_{avg,BV} = 0.45 \pm 0.13$ and 0.78 ± 0.14, respectively. This indicates that the smaller particles (measured at the higher SS) were higher in organic material. Little variance was seen between the control and acidified mesocosms.

Using the calculated kappa values, we determined the organic fraction using a kappa closure equation,

$$\kappa_{total} = \varepsilon_{org}\kappa_{org} + (1 - \varepsilon_{org})\kappa_{inorg} \quad (2)$$

where ε_{org} is the bulk volume fraction of organic material and κ is the kappa of the organic or inorganic material. Following Collins et al. (2013), we used $\kappa_{inorg} = 1.25$, a good proxy for seawater, and $\kappa_{org} = 0.006$. In BC, the organic fraction ranged from −0.21 to 0.46 (average, 0.24 ± 0.14) for SS = 0.39 %. For BV, the organic fraction ranged from 0.43–0.80 (average, 0.64 ± 0.11) for SS = 0.39 % and 0.19–0.55 (average, 0.38 ± 0.11) for SS = 0.08 %. Previous studies have also found mass organic fractions ranging from 30–80 % in sea spray aerosol studies of water from the Northern Atlantic, Sargasso Sea near Bermuda, and Pacific water near La Jolla, California (Collins et al., 2013; Facchini et al., 2008; Keene et al., 2007). Negative organic fractions were calculated during the BC campaign due to the sensitivity of Eq. (2) to the value of κ_{inorg} over κ_{org}. We show results here using a κ_{inorg} value supported by literature rather than determine non-realistic κ_{inorg} values to provide positive organic fractions. Therefore, the values shown in this work can be considered low estimates of the organic fraction. Table 3 shows average kappa and organic fraction values of each mesocosm for both campaigns.

ACPD
14, 26187–26230, 2014

The ratio of cloud condensation nuclei (CCN) to condensation nuclei (CN) decreased slightly during the pre-bloom period for SS = 0.39 %: at BC, CCN / $CN_{average}$ = 0.74 ± 0.03 whereas at BV, CCN / $CN_{average}$ = 0.65 ± 0.07. The change between CCN / CN during the oligotrophic and pre-bloom conditions was likely due to the combined effects of a higher organic fraction and higher Mode 2 to Mode 1 ratio during pre-bloom conditions, likely caused by the increasing organic content of the water due to the pre-bloom. For SS = 0.08 % measured at BV, CCN / $CN_{average}$ = 0.25 ± 0.04.

3.4 Correlations with biological parameters

In a recent study, Rinaldi et al. (2013) showed that chl *a* was the best biological surrogate for predicting organic enrichment in sea spray. Chl *a* parameterizations are currently being used in models to account for the organic content of seawater. We find a strong linear correlation with same-day measurements of organic fraction (from SS = 0.39 %) and total chl *a* concentrations (R^2 = 0.781) shown in Fig. 8, following

$$\text{Organic Fraction [\%]} = 42.28 \times (\text{chl } a)\ [\text{mg m}^{-3}] + 22.98 \quad (3)$$

Similar correlations were also found with a number of pigments: chlorophyll c1 + c2 (R^2 = 0.783), 19′-butanoyloxyfucoxanthin (R^2 = 0.711), alloxanthin (R^2 = 0.699), sum carotenes (R^2 = 0.773) and 19′-hexanoyloxyfucoxanthin (R^2 = 0.736) (Fig. 9). Various studies have found linear correlations between the organic fraction of aerosols measured at a receptor site and chl *a* concentrations observed by satellite along the back-trajectory (Langmann et al., 2008; O'Dowd et al., 2008; Rinaldi et al., 2013; Vignati et al., 2010); others have found exponential fittings (Gantt et al., 2011) with the same methodology or a Langmuir functional relationship (Long et al., 2011) using a model with experimental data from Facchini et al. (2008) and Keene et al. (2007). Figure 8 shows many of the existing chl *a*-organic fraction parameterizations in the literature, including this work. It is clear that many of the parameterizations from the Northern Atlantic Ocean also describe the correlation in the Mediterranean Sea fairly well, even

ACPD
14, 26187–26230, 2014

though the methodologies for most of them are very different from the one used in this study. The parameterization derived in this work is a high estimate when compared to the other parameterizations, even though it does not include a secondary organic contribution (contrary to satellite-receptor site studies). Consequently, organic components in Mediterranean primary marine aerosol are likely to be of multiple origins and not solely linked linearly to chl *a*-rich species. Bacteria have also been observed to affect the organic material in seawater (Gruber et al., 2006; Jiao et al., 2010; Ogawa et al., 2001). We find a correlation with heterotrophic prokaryotes ($R^2 = 0.476$), virus-like particles ($R^2 = 0.161$), autotrophic prokaryotes ($R^2 = 0.499$) and *Synechococcus* abundance ($R^2 = 0.143$), shown in Fig. 10a–d. In a wave channel experiment on natural seawater doped with Zobell growth medium, bacteria and phytoplankton (*Dunaliella tertiolecta*) cultures, Prather et al. (2013) also observed a link between heterotrophic bacteria and organic fraction while no correlation with chl *a* was found, highlighting the necessity to study complex systems of all biological material (phytoplankton, prokaryotes, organic matter) for marine aerosol. Most likely, the observed differences between Prather et al. (2013) and this work have to do with the localized biogeochemical nature of the different experiments, causing variance in the chemical composition and organic fraction of the marine aerosol. An additional correlation ($R^2 = 0.477$) exists with TEPs (Fig. 10e), a surface-active complex, variable mixture of organics (Filella, 2014; Passow, 2012). During BC, there is also a sigmoidal correlation between organic fraction and DOC concentrations ($\chi^2 = 0.411$); data are unavailable for BV (Fig. 10f).

We also wanted to see if correlations existed between different biogeochemical parameters and the temporal relative mode fractions shown in Fig. 2. Relative fractions of Modes 3 and 4 (91.5 and 260 nm, respectively) showed no clear correlations to any parameters. However, strong anti-correlations were observed between the Mode 1 (18.5 nm) relative fraction and the abundances and concentrations of virus-like particles, heterotrophic prokaryotes and all pigments previously discussed, except for alloxanthin, which had a positive correlation. The relative fraction of Mode 2 (37.5 nm) showed strong positive correlations with the abundances and concentrations of virus-

ACPD
14, 26187–26230, 2014

like particles, heterotrophic prokaryotes, TEPs and all the pigments discussed, except for alloxanthin, where no correlation was observed. This further supports the idea of an increase in the Mode 2 (Aitken mode) relative fraction during periods of high biological activity due to the higher concentrations of organic material, at the expense of Mode 1.

The control and acidified mesocosms showed no significant differences in terms of correlations between organic fraction and different biogeochemical parameters. For studies of marine aerosol, this indicates that any acidification effects on these biological parameters impacts the physical and chemical parameters of the aerosol much less than the natural variances caused by organic pre-bloom and bloom periods. It is not yet clear whether this observation can extend beyond the western Mediterranean Sea. However, it is important to note that due to the oligotrophic nature of the Mediterranean, even during the pre-bloom conditions at BV, the chl *a* concentrations and abundances of other parameters are still much lower than could occur in places like the North Atlantic Ocean.

4 Conclusions

By performing marine aerosol bubble-bursting experiments over two large-scale campaigns, we were able to compare the effects of ocean acidification during pre-bloom and oligotrophic conditions on physical and chemical properties of Mediterranean Sea aerosol. Ocean acidification had no direct effect on the physical parameters (size distribution, mode diameter and number fraction) measured in either campaign, with similar trends seen for all three differently acidified mesocosms.

Pre-bloom conditions at BV showed marked increases in the activation diameters and organic fractions (~ 64 %) for all the mesocosms at SS = 0.39 % compared to non-bloom conditions at BC (~ 24 %). At BV, larger particles (SS = 0.08 %) had smaller organic fractions (~ 38 %). Chl *a* and additional pigments were strongly correlated with the organic fraction, with weaker correlations observed with heterotrophic and autotrophic prokaryotes, virus-like particles, and *Synechococcus* abundances, and TEPs

ACPD
14, 26187–26230, 2014

and DOC concentrations. Many of these correlations corresponded specifically with the increase in Mode 2 (the Aitken mode) and were anti-correlated with Mode 1 during the pre-bloom period. The CCN / $CN_{average}$ ratio also decreased during the pre-bloom period at BV as a probable consequence of the increased organic content during a pre-bloom period. The parameterization of the primary marine aerosol organic fraction as a function of chl *a* derived in the present work is a high estimate of all the gathered parameterizations from the literature (with a higher organic fraction for a given chl *a* content), which may confirm that species other than chl *a*-rich species contribute to the organic content of marine aerosols in the Mediterranean atmosphere.

Author contributions. K. Sellegri, F. Gazeau, C. Guieu designed the experiments and A. N. Schwier, C. Rose, E. Asmi, K. Sellegri carried them out. Enriched microlayer data were provided by A. M. Ebling and W. M. Landing; pigment data were provided by A. Sallon and F. Gazeau; TEPs data were provided by S. Marro, M.-L. Pedrotti, F. Iuculano, and S. Agusti; bacteria and virus data were provided by S. Marro, M.-L. Pedrotti, A. Tsiola, and P. Pitta; and DOC data were provided by J. Louis and C. Guieu. A. N. Schwier and K. Sellegri prepared the manuscript with contributions from all co-authors.

Acknowledgements. This work was supported by the MISTRAL-CHARMEX project and by the EC FP7 project "Mediterranean Sea Acidification in a changing climate" (MedSeA; grant agreement 265103).

References

Albert, M. F. M. A., Schaap, M., Manders, A. M. M., Scannell, C., O'Dowd, C. D., and de Leeuw, G.: Uncertainties in the determination of global sub-micron marine organic matter emissions, Atmos. Environ., 57, 289–300, 2012.

Archer, S. D., Kimmance, S. A., Stephens, J. A., Hopkins, F. E., Bellerby, R. G. J., Schulz, K. G., Piontek, J., and Engel, A.: Contrasting responses of DMS and DMSP to ocean acidification in Arctic waters, Biogeosciences, 10, 1893–1908, doi:10.5194/bg-10-1893-2013, 2013.

Asa-Awuku, A., Engelhart, G. J., Lee, B. H., Pandis, S. N., and Nenes, A.: Relating CCN activity, volatility, and droplet growth kinetics of β-caryophyllene secondary organic aerosol, Atmos. Chem. Phys., 9, 795–812, doi:10.5194/acp-9-795-2009, 2009.

ACPD
14, 26187–26230, 2014

Asmi, E., Freney, E., Hervo, M., Picard, D., Rose, C., Colomb, A., and Sellegri, K.: Aerosol cloud activation in summer and winter at puy-de-Dôme high altitude site in France, Atmos. Chem. Phys., 12, 11589–11607, doi:10.5194/acp-12-11589-2012, 2012.

Ault, A. P., Moffet, R. C., Baltrusaitis, J., Collins, D. B., Ruppel, M. J., Cuadra-Rodriguez, L. A., Zhao, D., Guasco, T. L., Ebben, C. J., Geiger, F. M., Bertram, T. H., Prather, K. A., and Grassian, V. H.: Size-dependent changes in sea spray aerosol composition and properties with different seawater conditions, Environ. Sci. Technol., 47, 5603–5612, 2013.

Barger, W. R. and Garrett, W. D.: Surface Active Organic Material in the Marine Atmosphere, J. Geophys. Res., 75, 4561–4566, 1970.

Bates, T. S., Quinn, P. K., Frossard, A. A., Russell, L. M., Hakala, J., Petäjä, T., Kulmala, M., Covert, D. S., Cappa, C. D., Li, S.-M., Hayden, K. L., Nuaaman, I., Mclaren, R., Massoli, P., Canagaratna, M. R., Onasch, T. B., Sueper, D., Worsnop, D. R., and Keene, W. C.: Measurements of ocean derived aerosol off the coast of California, J. Geophys. Res., 117, D00V15, doi:10.1029/2012JD017588, 2012.

Benner, R.: Chemical composition and reactivity, in: Biogeochemistry of Marine Dissolved Organic Matter, edited by: Hansell, D. A. and Carlson, C. A., Academic Press, San Diego, CA, 59–90, 2002.

Bigg, E. K. and Leck, C.: The composition of fragments of bubbles bursting at the ocean surface, J. Geophys. Res., 113, D11209, doi:10.1029/2007JD009078, 2008.

Blanchard, D. C.: Sea-to-air transport surface active material, Science, 146, 396–397, 1964.

Blanchard, D. C. and Woodcock, A. H.: Bubble formation and modification in the sea and its meteorological significance, Tellus, 9 , 145–158, 1957.

Bosc, E., Bricaud, A., and Antoine, D.: Seasonal and interannual variability in algal biomass and primary production in the Mediterranean Sea, as derived from 4 years of SeaWiFS observations, Global Biogeochem. Cy., 18, GB1005, doi:10.1029/2003GB002034, 2004.

Callaghan, A. H., Deane, G. B., Stokes, M. D., and Ward, B.: Observed variation in the decay time of oceanic whitecap foam, J. Geophys. Res.-Oceans, 117, C09015, doi:10.1029/2012JC008147, 2012.

Cameron-Smith, P., Elliott, S., Maltrud, M., Erickson, D., and Wingenter, O.: Changes in dimethyl sulfide oceanic distribution due to climate change, Geophys. Res. Lett., 38, L07704, doi:10.1029/2011GL047069, 2011.

ACPD
14, 26187–26230, 2014

Clarke, A. D., Owens, S. R., and Zhou, J.: An ultrafine sea-salt flux from breaking waves: implications for cloud condensation nuclei in the remote marine atmosphere, J. Geophys. Res., 111, D06202, doi:10.1029/2005JD006565, 2006.

Collins, D. B., Ault, A. P., Moffet, R. C., Ruppel, M. J., Cuadra-Rodriguez, L. A., Guasco, T. L., Corrigan, C. E., Pedler, B. E., Azam, F., Aluwihare, L. I., Bertram, T. H., Roberts, G. C., Grassian, V. H., and Prather, K. A.: Impact of marine biogeochemistry on the chemical mixing state and cloud forming ability of nascent sea spray aerosol, J. Geophys. Res.Atmos., 118, 8553–8565, 2013.

Cunliffe, M., Engel, A., Frka, S., Gašparović, B., Guitart, C., Murrell, J. C., Salter, M., Stolle, C., Upstill-Goddard, R., and Wurl, O.: Sea surface microlayers: A unified physicochemical and biological perspective of the air–ocean interface, Prog. Oceanogr., 109, 104–116, 2013.

D'Ortenzio, F. and Ribera d'Alcalà, M.: On the trophic regimes of the Mediterranean Sea: a satellite analysis, Biogeosciences, 6, 139–148, doi:10.5194/bg-6-139-2009, 2009.

Danovaro, R., Corinaldesi, C., Dell'anno, A., Fuhrman, J. A., Middelburg, J. J., Noble, R. T., and Suttle, C. A.: Marine viruses and global climate change, FEMS Microbiol. Rev., 35, 993–1034, 2011.

Doney, S. C., Fabry, V. J., Feely, R. A., and Kleypas, J. A.: Ocean acidification: the other CO_2 problem, Ann. Rev. Marine Sci., 1, 169–192, 2009.

Ducklow, H. W., Carlson, C. A., Bates, N. R., Knap, A. H., Michaels, A. F., Jickells, T., Le, P. J., Williams, B., and McCave, I. N.: Dissolved organic carbon as a component of the biological pump in the North Atlantic Ocean, Philos. T. R. Soc. B, 348, 161–167, 1995.

Durrieu de Madron, X., Guieu, C., Sempéré, R., Conan, P., Cossa, D., D'Ortenzio, F., Estournel, C., Gazeau, F., Rabouille, C., Stemmann, L., Bonnet, S., Diaz, F., Koubbi, P., Radakovitch, O., Babin, M., Baklouti, M., Bancon-Montigny, C., Belviso, S., Bensoussan, N., Bonsang, B., Bouloubassi, I., Brunet, C., Cadiou, J. F., Carlotti, F., Chami, M., Charmasson, S., Charrière, B., Dachs, J., Doxaran, D., Dutay, J.-C., Elbaz-Poulichet, F., Eléaume, M., Eyrolles, F., Fernandez, C., Fowler, S., Francour, P., Gaertner, J. C., Galzin, R., Gasparini, S., Ghiglione, J. F., Gonzalez, J.-L., Goyet, C., Guidi, L., Guizien, K., Heimbürger, L.-E., Jacquet, S. H. M., Jeffrey, W. H., Joux, F., Le Hir, P., Leblanc, K., Lefèvre, D., Lejeusne, C., Lemé, R., Loÿe-Pilot, M.-D., Mallet, M., Méjanelle, L., Mélin, F., Mellon, C., Mérigot, B., Merle, P.-L., Migon, C., Miller, W. L., Mortier, L., Mostajir, B., Mousseau, L., Moutin, T., Para, J., Pérez, T., Petrenko, A., Poggiale, J.-C., Prieur, L., Pujo-Pay, M., Pulido-Villena, Raimbault, P., Rees, A. P., Ridame, C., Rontani, J.-F., Ruiz Pino, D., Sicre, M. A., Tail-

ACPD
14, 26187–26230, 2014

landier, V., Tamburini, C., Tanaka, T., Taupier-Letage, I., Tedetti, M., Testor, P., Thébault, H., Thouvenin, B., Touratier, F., Tronczynski, J., Ulses, C., Van Wambeke, F., Vantrepotte, V., Vaz, S., and Verney, R.: Marine ecosystems responses to climatic and anthropogenic forcings in the Mediterranean, Prog. Oceanogr., 91 , 97–166, 2011.

Engel, A.: Determination of marine gel particles, in: Practical Guidelines for the Analysis of Seawater, edited by: Wurl, O., CRC Press, Boca Raton, Florida, 125–142, 2009.

Facchini, M. C., Rinaldi, M., Decesari, S., Carbone, C., Finessi, E., Mircea, M., Fuzzi, S., Ceburnis, D., Flanagan, R., Nilsson, E. D., de Leeuw, G., Martino, M., Woeltjen, J., and O'Dowd, C. D.: Primary submicron marine aerosol dominated by insoluble organic colloids and aggregates, Geophys. Res. Lett., 35, L17814, doi:10.1029/2008GL034210, 2008.

Filella, M.: Understanding what we are measuring: standards and quantification of natural organic matter, Water Res., 50, 287–293, 2014.

Fuentes, E., Coe, H., Green, D., de Leeuw, G., and McFiggans, G.: Laboratory-generated primary marine aerosol via bubble-bursting and atomization, Atmos. Meas. Tech., 3, 141–162, doi:10.5194/amt-3-141-2010, 2010a.

Fuentes, E., Coe, H., Green, D., de Leeuw, G., and McFiggans, G.: On the impacts of phytoplankton-derived organic matter on the properties of the primary marine aerosol – Part 1: Source fluxes, Atmos. Chem. Phys., 10, 9295–9317, doi:10.5194/acp-10-9295-2010, 2010b.

Fuentes, E., Coe, H., Green, D., and McFiggans, G.: On the impacts of phytoplankton-derived organic matter on the properties of the primary marine aerosol – Part 2: Composition, hygroscopicity and cloud condensation activity, Atmos. Chem. Phys., 11, 2585–2602, doi:10.5194/acp-11-2585-2011, 2011.

Gantt, B. and Meskhidze, N.: The physical and chemical characteristics of marine primary organic aerosol: a review, Atmos. Chem. Phys., 13, 3979–3996, doi:10.5194/acp-13-3979-2013, 2013.

Gantt, B., Meskhidze, N., Facchini, M. C., Rinaldi, M., Ceburnis, D., and O'Dowd, C. D.: Wind speed dependent size-resolved parameterization for the organic mass fraction of sea spray aerosol, Atmos. Chem. Phys., 11, 8777–8790, doi:10.5194/acp-11-8777-2011, 2011.

Garrett, W. D.: The organic chemical composition of the ocean surface, Deep-Sea Res., 14 , 221–227, 1967.

Gazeau, F., Ziveri, P., Sallon, A., Lejeune, P., Gobert, S., Maugendre, L., Louis, J., Alliouane, S., Taillandier, V., Louis, F., Obolensky, G., Grisoni, J.-M., Delissanti, W., Luquet, D., Robin, D.,

ACPD
14, 26187–26230, 2014

Hesse, B., and Guieu, C.: First mesocosm experiments to study the impacts of ocean acidification on the plankton communities in the NW Mediterranean Sea (MedSeA project), in preparation, 2014.
Gruber, D. F., Simjouw, J.-P., Seitzinger, S. P., and Taghon, G. L.: Dynamics and characterization of refractory dissolved organic matter produced by a pure bacterial culture in an experimental predator-prey system, Appl. Environ. Microb., 72, 4184–4191, 2006.
Grythe, H., Ström, J., Krejci, R., Quinn, P., and Stohl, A.: A review of sea-spray aerosol source functions using a large global set of sea salt aerosol concentration measurements, Atmos. Chem. Phys., 14, 1277–1297, doi:10.5194/acp-14-1277-2014, 2014.
Guieu, C., Dulac, F., Ridame, C., and Pondaven, P.: Introduction to project DUNE, a DUst experiment in a low Nutrient, low chlorophyll Ecosystem, Biogeosciences, 11, 425–442, doi:10.5194/bg-11-425-2014, 2014.
Hansell, D. A., Carlson, C. A., Repeta, D. J., and Schlitzer, R.: Dissolved organic matter in the ocean, Oceanography, 22, 202–211, 2009.
Hultin, K., Nilsson, E. D., Krejci, R., Mårtensson, E. M., Ehn, M., Hagström, Å., and de Leeuw, G.: In situ laboratory sea spray production during the Marine Aerosol Production 2006 cruise on the northeastern Atlantic Ocean, J. Geophys. Res., 115, D06201, doi:10.1029/2009JD012522, 2010.
Hultin, K., Krejci, R., Pinhassi, J., Gomez-Consarnau, L., Mårtensson, E. M., Hagström, Å., and Nilsson, E. D.: Aerosol and bacterial emissions from Baltic Seawater, Atmos. Res., 99 , 1–14, 2011.
Jiao, N., Herndl, G. J., Hansell, D. A., Benner, R., Kattner, G., Wilhelm, S. W., Kirchman, D. L., Weinbauer, M. G., Luo, T., Chen, F., and Azam, F.: Microbial production of recalcitrant dissolved organic matter: long-term carbon storage in the global ocean, Nat. Rev. Microbiol., 8, 593–599, 2010.
Keene, W. C., Maring, H., Maben, J. R., Kieber, D. J., Pszenny, A. A. P., Dahl, E. E., Izaguirre, M. A., Davis, A. J., Long, M. S., Zhou, X., Smoydzin, L., and Sander, R.: Chemical and physical characteristics of nascent aerosols produced by bursting bubbles at a model air-sea interface, J. Geophys. Res., 112, D21202, doi:10.1029/2007JD008464, 2007.
King, S. M., Butcher, A. C., Rosenoern, T., Coz, E., Lieke, K. I., de Leeuw, G., Nilsson, E. D., and Bilde, M.: Investigating primary marine aerosol properties: CCN activity of sea salt and mixed inorganic-organic particles, Environ. Sci. Technol., 46, 10405–10412, 2012.

ACPD
14, 26187–26230, 2014

Langmann, B., Scannell, C., and O'Dowd, C.: New directions: organic matter contribution to marine aerosols and cloud condensation nuclei, Atmos. Environ., 42, 7821–7822, 2008.
Lewis, S. and Schwartz, R.: Sea Salt Aerosol Production: Mechanisms, Methods, Measurements, and Models – A Critical Review, American Geophysical Union, Washington, DC, 1–413, 2004.
Lion, L. W. and Leckie, J. O.: The biogeochemistry of the air-sea interface, Annu. Rev. Earth Pl. Sc., 9, 449–486, 1981.
Long, M. S., Keene, W. C., Kieber, D. J., Erickson, D. J., and Maring, H.: A sea-state based source function for size- and composition-resolved marine aerosol production, Atmos. Chem. Phys., 11, 1203–1216, doi:10.5194/acp-11-1203-2011, 2011.
Mårtensson, E. M., Nilsson, E. D., de Leeuw, G., Cohen, L. H., and Hansson, H.-C.: Laboratory simulations and parameterization of the primary marine aerosol production, J. Geophys. Res., 108, 4297, doi:10.1029/2002JD002263, 2003.
Matrai, P. A., Tranvik, L., Leck, C., and Knulst, J. C.: Are high Arctic surface microlayers a potential source of aerosol organic precursors?, Mar. Chem., 108, 109–122, 2008.
Moore, M. J. K., Furutani, H., Roberts, G. C., Moffet, R. C., Gilles, M. K., Palenik, B., and Prather, K. A.: Effect of organic compounds on cloud condensation nuclei (CCN) activity of sea spray aerosol produced by bubble bursting, Atmos. Environ., 45, 7462–7469, 2011.
Murphy, D. M., Anderson, J. R., Quinn, P. K., McInnes, L. M., Brechtel, F. J., Kreidenweis, S. M., Middlebrook, A. M., Pósfai, M., Thomson, D. S., and Buseck, P. R.: Influence of sea-salt on aerosol radiative properties in the Southern Ocean marine boundary layer, Nature, 392, 62–65, 1998.
O'Dowd, C. D., Facchini, M. C., Cavalli, F., Ceburnis, D., Mircea, M., Decesari, S., Fuzzi, S., Yoon, Y. J., and Putaud, J.-P.: Biogenically driven organic contribution to marine aerosol, Nature, 431, 676–680, 2004.
O'Dowd, C. D., Langmann, B., Varghese, S., Scannell, C., Ceburnis, D., and Facchini, M. C.: A combined organic-inorganic sea-spray source function, Geophys. Res. Lett., 35, L01801, doi:10.1029/2007GL030331, 2008.
Ogawa, H., Amagai, Y., Koike, I., Kaiser, K., and Benner, R.: Production of refractory dissolved organic matter by bacteria, Science, 292, 917–920, 2001.
Passow, U.: The abiotic formation of TEP under different ocean acidification scenarios, Mar. Chem., 128–129, 72–80, 2012.

ACPD
14, 26187–26230, 2014

Petters, M. D. and Kreidenweis, S. M.: A single parameter representation of hygroscopic growth and cloud condensation nucleus activity, Atmos. Chem. Phys., 7, 1961–1971, doi:10.5194/acp-7-1961-2007, 2007.

Prather, K. A., Bertram, T. H., Grassian, V. H., Deane, G. B., Stokes, M. D., Demott, P. J., Aluwihare, L. I., Palenik, B. P., Azam, F., Seinfeld, J. H., Moffet, R. C., Molina, M. J., Cappa, C. D., Geiger, F. M., Roberts, G. C., Russell, L. M., Ault, A. P., Baltrusaitis, J., Collins, D. B., Corrigan, C. E., Cuadra-Rodriguez, L. A., Ebben, C. J., Forestieri, S. D., Guasco, T. L., Hersey, S. P., Kim, M. J., Lambert, W. F., Modini, R. L., Mui, W., Pedler, B. E., Ruppel, M. J., Ryder, O. S., Schoepp, N. G., Sullivan, R. C., and Zhao, D.: Bringing the ocean into the laboratory to probe the chemical complexity of sea spray aerosol, P. Natl. Acad. Sci. USA, 110, 7550–7555, 2013.

Pringle, K. J., Tost, H., Pozzer, A., Pöschl, U., and Lelieveld, J.: Global distribution of the effective aerosol hygroscopicity parameter for CCN activation, Atmos. Chem. Phys., 10, 5241–5255, doi:10.5194/acp-10-5241-2010, 2010.

Quinn, P. K. and Bates, T. S.: The case against climate regulation via oceanic phytoplankton sulphur emissions, Nature, 480, 51–56, 2011.

Riebesell, U. and P. D. Tortell, Effects of ocean acidification on pelagic organisms and ecosystems., in: Ocean Acidification, edited by: Gattuso, J. P. and Hansson, L., Oxford University Press, Oxford, 99–121, 2011.

Rinaldi, M., Fuzzi, S., Decesari, S., Marullo, S., Santoleri, R., Provenzale, A., von Hardenberg, J., Ceburnis, D., Vaishya, A., O'Dowd, C. D., and Facchini, M. C.: Is chlorophyll *a* the best surrogate for organic matter enrichment in submicron primary marine aerosol?, J. Geophys. Res.-Atmos., 118, 4964–4973, 2013.

Roberts, G. C. and Nenes, A.: A continuous-flow streamwise thermal-gradient CCN chamber for atmospheric measurements, Aerosol Sci. Tech., 39, 206–221, 2005.

Russell, L. M., Hawkins, L. N., Frossard, A., Quinn, P. K., and Bates, T. S.: Carbohydrate-like composition of submicron atmospheric particles and their production from ocean bubble bursting, P. Natl. Acad. Sci. USA, 107, 6652–6657, 2010.

Sciare, J., Mihalopoulos, N., and Dentener, F. J.: Interannual variability of atmospheric dimethylsulfide in the southern Indian Ocean, J. Geophys. Res., 105, 26369–26377, 2000.

Sciare, J., Favez, O., Sarda-Estève, R., Oikonomou, K., Cachier, H., and Kazan, V.: Long-term observations of carbonaceous aerosols in the Austral Ocean atmosphere: evidence of a bio-

ACPD
14, 26187–26230, 2014

genic marine organic source, J. Geophys. Res., 114, D15302, doi:10.1029/2009JD011998, 2009.
Sellegri, K., O'Dowd, C. D., Yoon, Y. J., Jennings, S. G., and de Leeuw, G.: Surfactants and submicron sea spray generation, J. Geophys. Res., 111, D22215, doi:10.1029/2005JD006658, 2006.
Siokou-Frangou, I., Christaki, U., Mazzocchi, M. G., Montresor, M., Ribera d'Alcalá, M., Vaqué, D., and Zingone, A.: Plankton in the open Mediterranean Sea: a review, Biogeosciences, 7, 1543–1586, doi:10.5194/bg-7-1543-2010, 2010.
Spracklen, D. V., Arnold, S. R., Sciare, J., Carslaw, K. S., and Pio, C.: Globally significant oceanic source of organic carbon aerosol, Geophys. Res. Lett., 35, L12811, doi:10.1029/2008GL033359, 2008.
Stommel, Y. G. and Riebel, U.: A new corona discharge-based aerosol charger for submicron particles with low initial charge, J. Aerosol Sci., 35, 1051–1069, 2004.
Stommel, Y. G. and Riebel, U.: A corona-discharge-based aerosol neutralizer designed for use with the SMPS-system, J. Electrostat., 63, 917–921, 2005.
Tyree, C. A., Hellion, V. M., Alexandrova, O. A., and Allen, J. O.: Foam droplets generated from natural and artificial seawaters, J. Geophys. Res., 112, D12204, doi:10.1029/2006JD007729, 2007.
Vignati, E., Facchini, M. C., Rinaldi, M., Scannell, C., Ceburnis, D., Sciare, J., Kanakidou, M., Myriokefalitakis, S., Dentener, F., and O'Dowd, C. D.: Global scale emission and distribution of sea-spray aerosol: sea-salt and organic enrichment, Atmos. Environ., 44, 670–677, 2010.
Weinbauer, M. G., Mari, X., and Gattuso, J.-P.: Effect of ocean acidification on the diversity and activity of heterotrophic marine microorganisms, in: Ocean Acidification, edited by: Gattuso, J.-P. and Hansson, L., Oxford University Press, Oxford, 83–98, 2011.
Woodhouse, M. T., Mann, G. W., Carslaw, K. S., and Boucher, O.: Sensitivity of cloud condensation nuclei to regional changes in dimethyl-sulphide emissions, Atmos. Chem. Phys., 13, 2723–2733, doi:10.5194/acp-13-2723-2013, 2013.
Yoon, Y. J., Ceburnis, D., Cavalli, F., Jourdan, O., Putaud, J. P., Facchini, M. C., Decesari, S., Fuzzi, S., Sellegri, K., Jennings, S. G., and O'Dowd, C. D.: Seasonal characteristics of the physicochemical properties of North Atlantic marine atmospheric aerosols, J. Geophys. Res., 112, D04206, doi:10.1029/2005JD007044, 2007.
Zábori, J., Krejci, R., Ekman, A. M. L., Mårtensson, E. M., Ström, J., de Leeuw, G., and Nilsson, E. D.: Wintertime Arctic Ocean sea water properties and primary marine aerosol

ACPD
14, 26187–26230, 2014

concentrations, Atmos. Chem. Phys., 12, 10405–10421, doi:10.5194/acp-12-10405-2012, 2012a.

Zábori, J., Matisāns, M., Krejci, R., Nilsson, E. D., and Ström, J.: Artificial primary marine aerosol production: a laboratory study with varying water temperature, salinity, and succinic acid concentration, Atmos. Chem. Phys., 12, 10709–10724, doi:10.5194/acp-12-10709-2012, 2012b.

ACPD

14, 26187–26230, 2014

Table 1. Calibration information at varying temperature gradients for NaCl (35 g L^{-1}) in tank.

Temperature Gradient	Activation Diameter (nm)	Supersaturation (%)
d*T*6	42.497 ± 1.82	0.39
d*T*3	122.915 ± 8.65	0.08

ACPD
14, 26187–26230, 2014

Table 2. Modal diameters (nm) and number fractions from the size distributions for both campaigns, including data from both supersaturations and enriched experiments. Lognormal modal diameters and number fractions from Fuentes et al. (2010a) are also shown.

	BC (SS = 0.39 % and enriched)		BV (SS = 0.39 + 0.08 % and enriched)		Artificial Sea Water Fuentes et al. (2010)	
	Diameter	Fraction	Diameter	Fraction	Diameter	Fraction
Mode 1	17	0.323	20	0.193	14	0.382
Mode 2	38	0.295	37	0.482	48	0.317
Mode 3	91	0.268	92	0.241	124	0.168
Mode 4	260	0.114	260	0.084	334	0.133

ACPD
14, 26187–26230, 2014

Table 3. Average activation diameters, kappa values and organic fractions for both campaigns and supersaturations.

		Mesocosm	Activation Diameter (nm)	κ	Organic Fraction
BC	SS = 0.39 %	C3	47.475 ± 1.56	0.884 ± 0.107	0.294 ± 0.086
		C3, enriched	46.782 ± 4.07	0.924 ± 0.084	0.262 ± 0.068
		P3	45.761 ± 1.77	1.001 ± 0.191	0.200 ± 0.156
		P3, enriched	48.869 ± 6.09	0.81 ± 0	0.354 ± 0
		P6	45.714 ± 1.62	1.003 ± 0.230	0.199 ± 0.185
		P6, enriched	46.691 ± 3.39	0.931 ± 0.080	0.257 ± 0.064
BV	SS = 0.39 %	C3	61.831 ± 2.22	0.404 ± 0.086	0.680 ± 0.069
		C3, enriched	51.901 ± 4.77	0.676 ± 0	0.461 ± 0
		P3	61.217 ± 2.10	0.411 ± 0.123	0.674 ± 0.099
		P6	59.074 ± 1.89	0.465 ± 0.152	0.631 ± 0.122
		P6, enriched	53.918 ± 3.63	0.609 ± 0.103	0.516 ± 0.083
		Outside	54.225 ± 3.65	0.593 ± 0.137	0.528 ± 0.110
		Outside, enriched	55.527 ± 2.99	0.551 ± 0.066	0.562 ± 0.053
	SS = 0.08 %	C3	146.040 ± 16.60	0.718 ± 0.143	0.427 ± 0.115
		C3, enriched	148.487 ± 37.10	0.687 ± 0	0.453 ± 0
		P6	137.14 ± 15.50	0.867 ± 0.132	0.308 ± 0.106

ACPD
14, 26187–26230, 2014

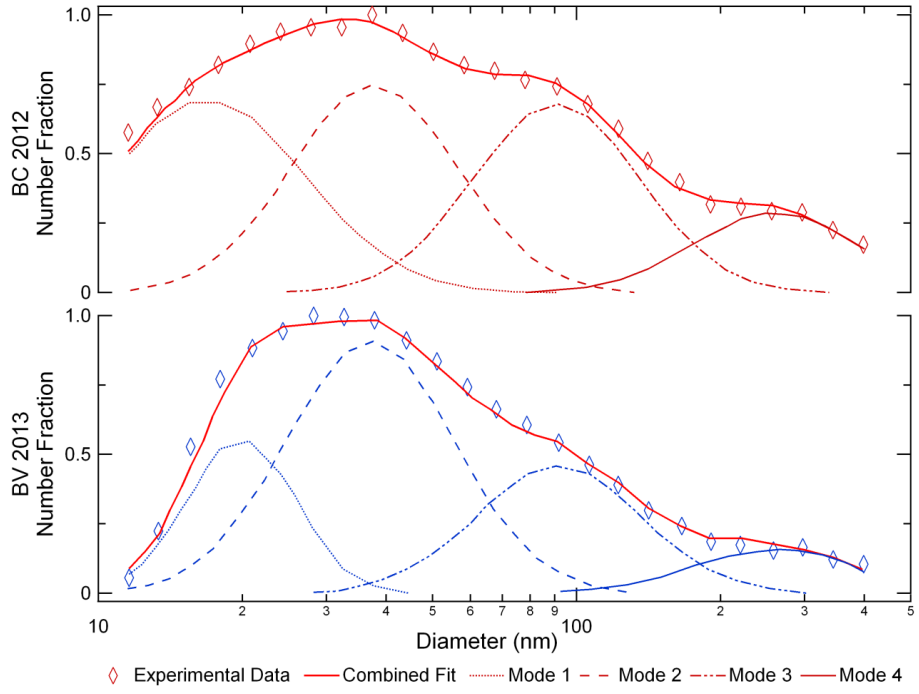

Figure 1. Average size distributions for each campaign (Bay of Calvi, BC, and Bay of Villefranche, BV) fit with 4 lognormal modes. Each campaign average is taken from the supersaturations (SS = 0.08 and 0.39 %) used for all three mesocosms and includes all enriched samples as well.

ACPD
14, 26187–26230, 2014

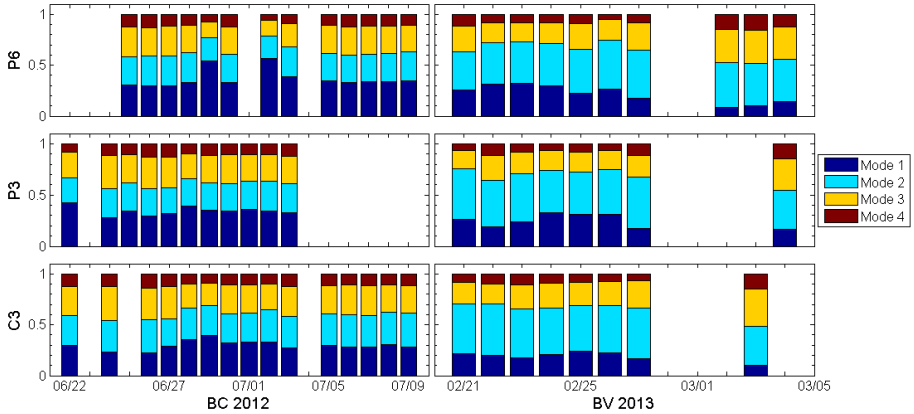

Figure 2. Number fraction of DMPS lognormal modes from all mesocosms (SS = 0.39 %) at BC and BV.

ACPD
14, 26187–26230, 2014

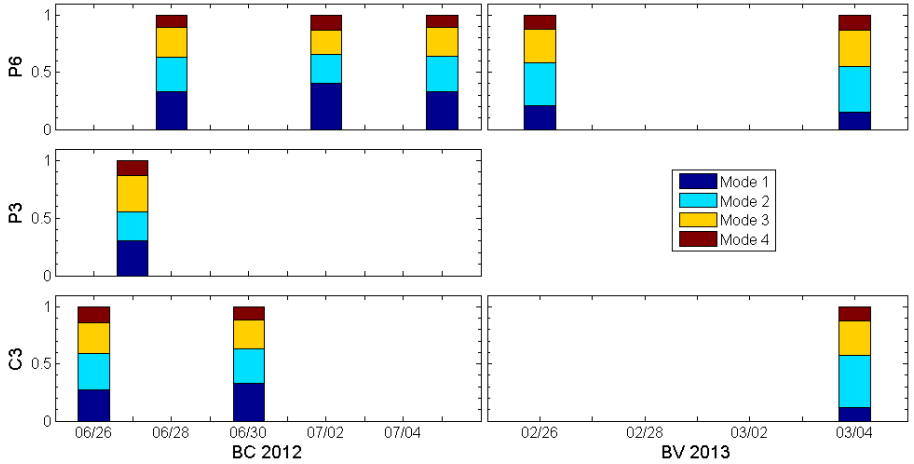

Figure 3. Number fraction of DMPS lognormal modes from enriched samples (SS = 0.39 %) at BC and BV.

ACPD
14, 26187–26230, 2014

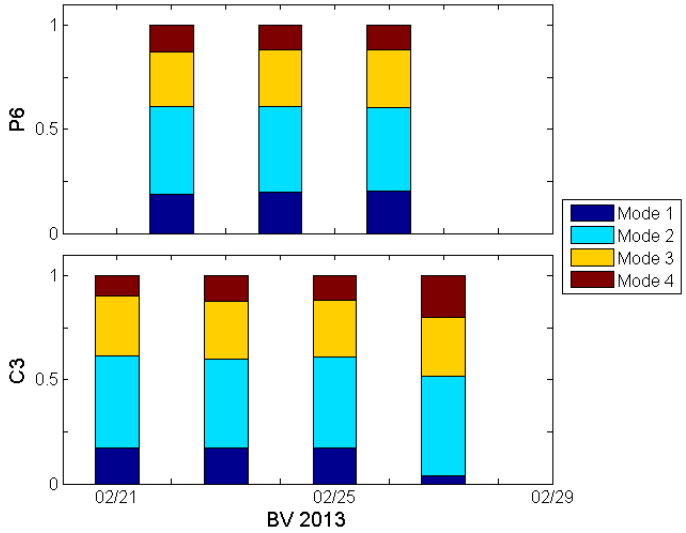

Figure 4. Number fraction of DMPS lognormal modes tested at SS = 0.08 % for mesocosms C3 and P6 at BV.

ACPD
14, 26187–26230, 2014

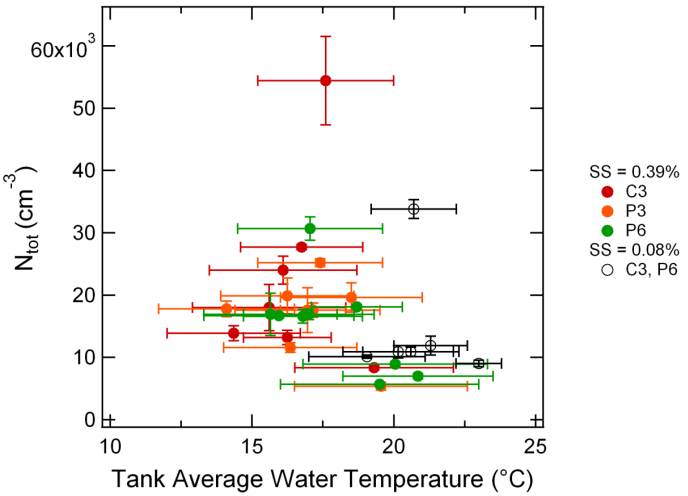

Figure 5. Number concentration vs. the average tank water temperature from BV for both supersaturations tested.

ACPD
14, 26187–26230, 2014

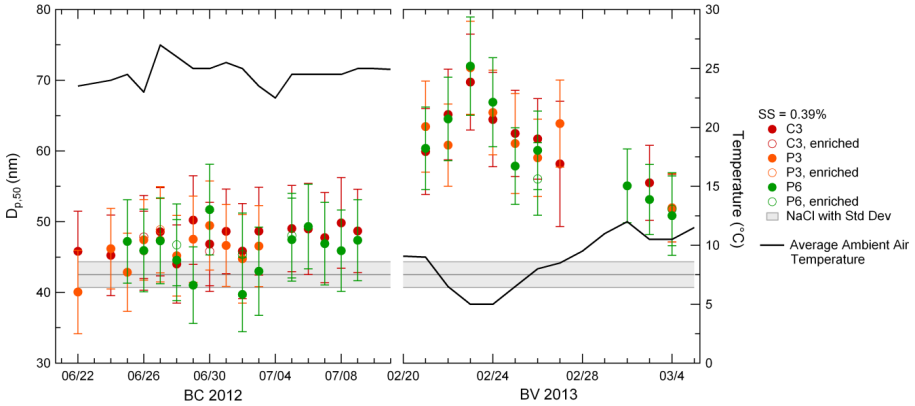

Figure 6. Activation diameter and ambient air temperatures for BC and BV. Data is shown for SS = 0.39 % (d*T*6), including the enriched experiments. The shaded bar indicates the NaCl activation diameter at the given supersaturation.

ACPD
14, 26187–26230, 2014

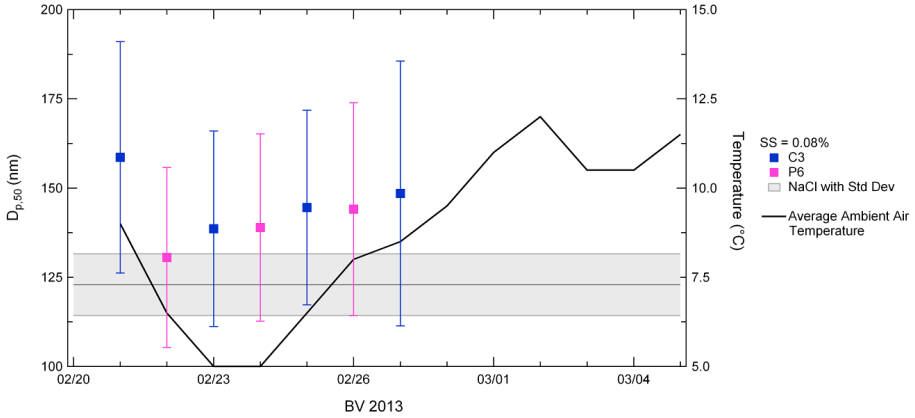

Figure 7. Activation diameter and ambient air temperatures for BV. Data is shown for SS = 0.08 % (d*T*3). The shaded bar indicates the NaCl activation diameter.

ACPD
14, 26187–26230, 2014

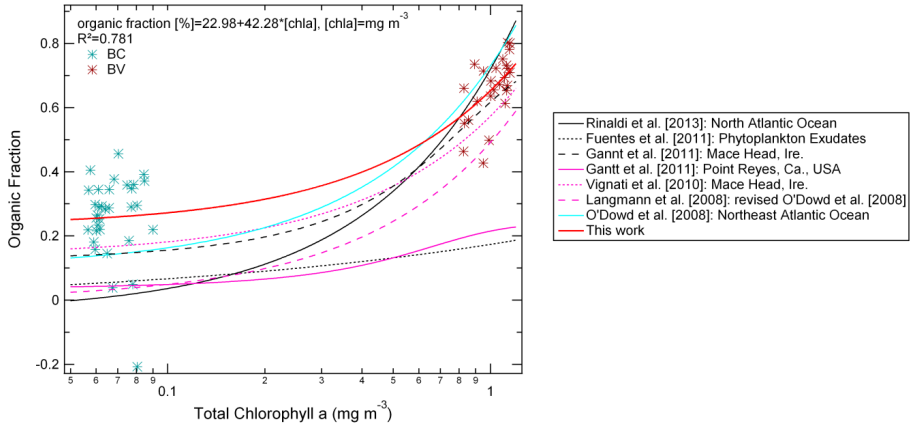

Figure 8. Organic fraction calculated from kappa (κ_{org} = 0.006 and κ_{inorg} = 1.25) at SS = 0.39 % vs. total chlorophyll *a* concentrations (mg m^{-3}) for all 3 mesocosms during both BC and BV, fit with published parameterizations of the organic fraction–chl *a* relationship.

ACPD
14, 26187–26230, 2014

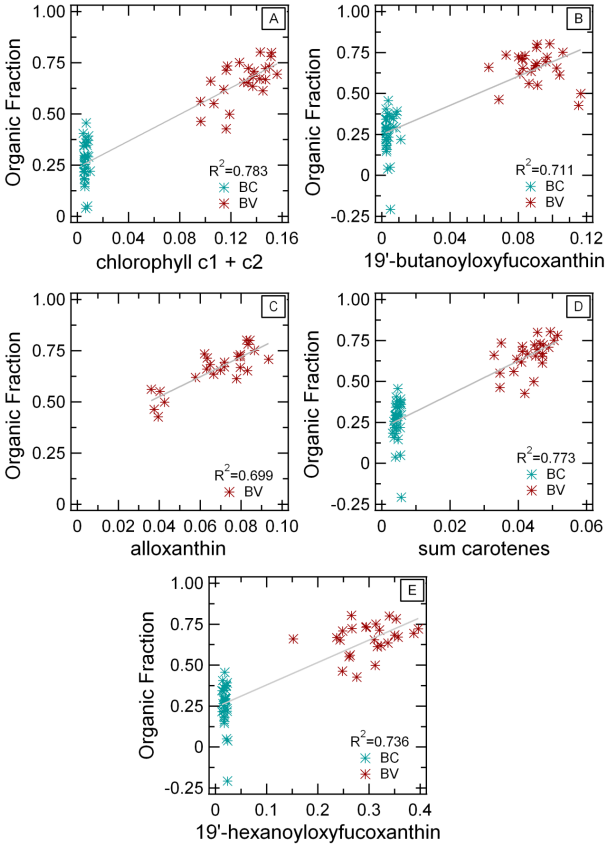

Figure 9. Organic fraction calculated from kappa (κ_{org} = 0.006 and κ_{inorg} = 1.25) at SS = 0.39 % vs. chlorophyll c1 + c2 **(A)**, 19′-butanoyloxyfucoxanthin **(B)**, alloxanthin **(C)**, sum carotenes **(D)** and 19′-hexanoyloxyfucoxanthin **(E)** concentrations (mg m^{-3}) for all 3 mesocosms during both BC and BV. Linear fits with R^2 values are shown for all figures.

ACPD
14, 26187–26230, 2014

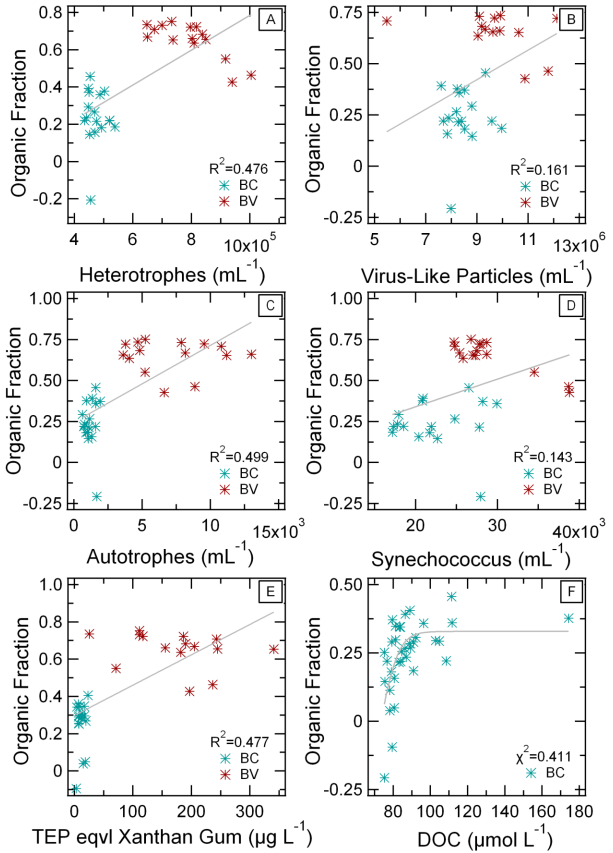

Figure 10. Organic fraction calculated from kappa ($\kappa_{org} = 0.006$ and $\kappa_{inorg} = 1.25$) at SS = 0.39 % vs. heterotrophic prokaryotes **(A)**, virus-like particles **(B)**, autotrophic prokaryotes **(C)**, and *Synechococcus* **(D)** abundances, and TEP equivalent (xanthan gum) **(E)**, and DOC **(F)** concentrations for all 3 mesocosms during both BC and BV. Linear fits with R^2 values are shown for all figures except for **(F)**, which is shown with a sigmoid fit and χ^2 value.

ACPD
14, 26187–26230, 2014